International Journal of Control and Automation
Vol.8, No.10 (2015), pp.109-124
http://dx.doi.org/10.14257/ijca.2015.8.10.11

Energy Consumption Modeling and Optimization of Traction Control for High-speed Railway Trains

Jiang Liu[1, 2]*, Bai-gen Cai[1], Gang Xu[3] and Gao-feng Sun[3]

1 School of Electronic and Information Engineering, Beijing Jiaotong University, Beijing 100044, China
2 State Key Laboratory of Rail Traffic Control and Safety, Beijing Jiaotong University, Beijing 100044, China
3 CSR Sifang Locomotive and Rolling Stock Co. Ltd., Qingdao 266111, China
**E-mail: jiangliu@bjtu.edu.cn*

Abstract

The energy consumption modeling and the optimization solution for the traction control of high-speed trains are addressed in this paper. Based on the analysis of the operation process, an improved train traction analysis with the multi-mass modeling approach is presented, and the corresponding energy consumption model is investigated. By considering the issues of the passenger comfort and traveling time, an optimization algorithm for traction control of the high-speed trains is presented by using a multi-objective-fitness particle swarm optimization technique. Simulations are performed with practical parameters of the CRH EMU (Electric Multiple Unit) and railway line, and the results demonstrate the performance of the proposed solution over the conventional traction calculation method.

Keywords: *High-Speed Railway; Traction Control; Multi-Mass EMU Model; Energy-Efficient Control; Particle Swarm Optimization; Multi-Objective Optimization*

1. Introduction

In recent years, the high-speed railway in China is experiencing a rapid development based on an ambitious plan for the future railway transportation architecture, and operation length of the high-speed railway in China by the end of 2013 has reached 50% of the total length in the world [1,2]. Besides railway infrastructures, the high-speed Electronic Multiple Units (EMUs) are the decisive elements that undertake the supplement of transport capabilities. In the past decade, Chinese Train Control System (CTCS) was established and became a comprehensive system for the operation control, dispatching and safety assurance of EMUs [3]. Considering the optimization of transport services in a system level, there have been several key aspects addressed, including the traffic safety, efficiency, environmental friendliness, and multimodal interoperability, etc. Among these issues, the energy efficiency is another significant factor in the design and optimization of the railway operations, especially the energy consumption of each individual train [4]. The energy consumption of traction control for the high-speed trains depends on the train's configuration, propulsion system, traction current, and the operation conditions. Since the trains have to operate according to plans from the railway dispatching system, the planned trajectories, which are used as the inputs to the driver guidance system or an automatic control system, describe the permitted motion of the trains, and hence the energy consumption could be identified and optimized from the planning of trajectories [5].

From the view of train trajectory optimization when considering the energy saving problem of traction control, there have been many results by the researchers and engineers.

ISSN: 2005-4297 IJCA
Copyright ⓒ 2015 SERSC

Moritani [6] analyzed the trade off relation between the total consumed energy, the running time, the loss of traction motors and inverters. Feng [7] summarized the traction energy cost and transport operation time of high-speed trains with a range of target speeds through simulations. Li [8] proposed a green train scheduling model and fuzzy multi-objective optimization algorithm to minimize the energy consumption, where the similar approaches can be found in [9,10]. For pursuing an identified effect for the trajectory or the speed-curve, some intelligent methods, including genetic algorithm [11], swarm intelligence [12] and neural network [13], have been introduced and improved in the energy efficient solutions. However, besides the assurance of energy efficiency, it is expected to achieve a comprehensive effect concerning several aspects based on a considerable level of energy capability, which means the adaptability, precision of the traction model and computation efficiency of the solution should also be concerned.

In this paper, we focus on the traction energy consumption modeling of high-speed trains. A multi-mass approach is adopted to generate an optimized traction control solution by using the Particle Swarm Optimization (PSO) technique with an improved fitness. Simulations are performed to demonstrate the capability and potential of the proposed solution. The rest of this paper is organized as follows. Section 2 details the train traction model using PSO, and the results and discussions are given in Section 3. Finally, Section 4 concludes this paper.

2. Design of Traction Control Method

2.1. Traction Model and Energy Consumption Analysis

The practical operation of a high-speed train corresponds to several issues, including the traction control, the dynamic characteristics of the train, the rail signaling control conditions and the experience and status of the drivers, etc. In order to evaluate and optimize the train operation process, the kinematic model of the high-speed trains is essential to provide an effective approach. Although there are some differences between CRH EMU and the existing railway locomotives [14], the stress condition and operation characteristics of the trains can be analyzed according to the Newton's second law.

Considering the operation modes of a CRH train and its force analysis, the resultant force is derived from the integration of the traction force, the braking force and the resistance force. The practical force situation of a train is determined by the operating condition concerning the kinematical limits, rail track situations and the operation conditions. A typical CRH train operation process can be divided into three operation conditions, where Figure 1 shows the speed-distance curve between two adjacent railway stations.

(1) Traction condition

The resultant force of the train is calculated through an integration of the traction force and the resistance, where the train's speed increases with the running distance (e.g. b_0-b_1, b_4-b_5).

(2) Braking condition

The brake force and resistance contribute to a decreased train speed under the pull-into or the braking scenarios (e.g. b_2-b_3, b_6-b_7).

(3) Intermediate condition

The intermediate condition is used for keeping the train speed within a range from a lower bound to an upper bound, where the coasting or cruising could be involved (e.g. b_1-b_2, b_3-b_4, b_5-b_6). This is an indispensable procedure between the traction and braking conditions.

 Copyright ⓒ 2015 SERSC

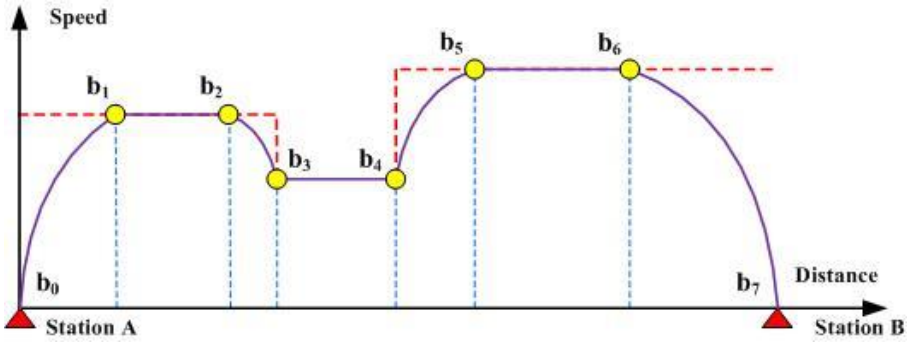

Figure 1. Speed-Distance Curve of a Whole Trip between Two Stations

Based on the above mentioned principle, all the operation conditions and corresponding force situations should be concentrated in the traction modeling process. Hence, the kinematic model of a high-speed train can be written as

$$v\frac{dv}{dx} = u_{\mathrm{t}} f(v) - u_{\mathrm{b}} b(v) - r(v) - g(x,v) \tag{1}$$

where v represents the train speed, x is traveling distance from a certain reference track location, $u_{\mathrm{t}}(0 \le u_{\mathrm{t}} \le 1)$ and $u_{\mathrm{b}}(-1 \le u_{\mathrm{b}} \le 0)$ denote the traction coefficient and braking coefficient, and $\{f(v), b(v), r(v), g(x,v)\}$ are traction force, braking force, basic resistance and the additional resistance, respectively.

In most traditional results of force analysis and kinematic modeling, only a single particle model is concerned for pursuing the simplicity and calculation efficiency. However, with a high resolution for analyzing the kinematics of the high-speed railway trains, the multi-mass EMU model is definitely required to illustrate the inherent mechanism. When using a CRH-2 EMU as an example, which usually consists of 8 compartments including 4 motor units and 4 trailer units, the multi-mass model can be achieved as shown in Figure 2.

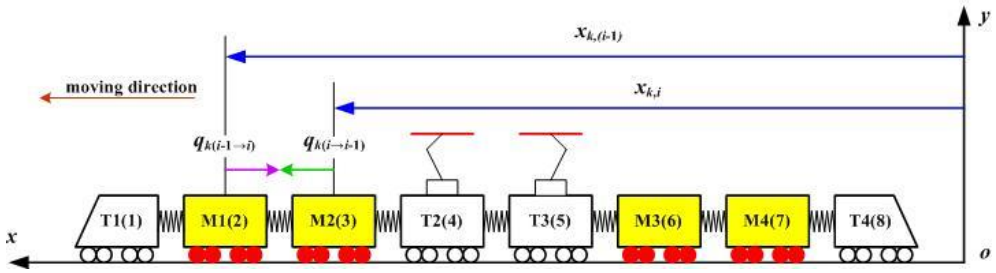

Figure 2. Force Analysis of an EMU using the Multi-Mass Model

At instant k, the resultant force of compartment i can be calculated as

$$F_{ki} = u_{\mathrm{t}} f(v_{ki}) - u_{\mathrm{b}} b(v_{ki}) - W_{ki} + Q_{ki} \tag{2}$$

$$Q_{ki} = \begin{cases} q_{k(i+1\to i)} & i = 1 \\ q_{k(i-1\to i)} & i = 8 \\ q_{k(i-1\to i)} + q_{k(i+1\to i)} & i = 2,\cdots,7 \end{cases} \tag{3}$$

Copyright ⓒ 2015 SERSC

$$q_{k(i-1\to i)} = \varepsilon_{i-1,i}\left(x_{ki} - x_{k(i-1)}\right) \tag{4}$$

where W_{ki} denotes the resistance force for the i th train compartment which is an integration of the basic and additional resistance, $q_{k(i\to j)}$ represents the interaction force between two adjacent compartments from i to $j(j = i-1, i+1)$, $\varepsilon_{i-1,i}$ is the elasticity coefficient between two compartments, and x_{ki} denotes the 1D location of compartment i at instant k.

Thus, the acceleration of the train compartment i is

$$a_{ki} = \frac{F_{ki}}{(1+\gamma)m_{ki}} \tag{5}$$

where γ is the rotary mass coefficient which is always set 0.06, and m_{ki} denotes the weight of the i th compartment at instant k.

When considering the train as a rigid body and the damping is ignored, each compartment is supposed to have the same acceleration as the whole EMU, which means that

$$a_{k1} = a_{k2} = \cdots = a_{k8} = a_k \tag{6}$$

Therefore, the interaction forces fulfill the following constraints when we just consider the longitudinal force, where

$$q_{k(i-1\to i)} + q_{k(i\to i-1)} = 0 \tag{7}$$

Under this circumstance, the force analysis of the whole EMU is realized by integrating the resultant force of all the compartments, which means that

$$\begin{aligned} F_k &= \sum_{i=1}^{8} F_{ki} = (1+\gamma)a_k \sum_{i=1}^{8} m_{ki} = u_{\mathrm{t}} f(v_{k1}) - u_{\mathrm{b}} b(v_{k1}) - W_{k1} + q_{k(2\to 1)} \\ &\quad + \sum_{j=2}^{7}\left\{u_{\mathrm{t}} f(v_{kj}) - u_{\mathrm{b}} b(v_{kj}) - W_{kj} + q_{k(j-1\to j)} + q_{k(j+1\to j)}\right\} + u_{\mathrm{t}} f(v_{k8}) \\ &\quad - u_{\mathrm{b}} b(v_{k8}) - W_{k8} + q_{k(7\to 8)} \\ &= \sum_{j=2,3,6,7}\left\{u_{\mathrm{t}} f(v_{kj})\right\} - \sum_{i=1}^{8}\left\{u_{\mathrm{b}} b(v_{ki}) + W_{ki}\right\} \end{aligned} \tag{8}$$

The Eq. (8) shows a simplified multi-mass model of the CRH-2 EMU where the relative motion of two adjacent compartments, which can be represented by the relative displacement $\Delta x_{i-1,i}(i = 2,\cdots,7)$ according to $m_i \Delta \ddot{x}_{i-1,i}$, is replaced by the rigid body as Eq. (6). With the resultant force analysis, the train traction model could be derived according to the different conditions, where the traction, braking, coasting and cruising conditions are concerned. Here we use the traction acceleration a_k^f to describe the traction control strategies.

 Copyright ⓒ 2015 SERSC

$$a_k^f = \begin{cases} a_k - \dfrac{\sum_{i=1}^{8} W_{ki}}{(1+\gamma)\sum_{i=1}^{8} m_{ki}} & traction \\ 0 & braking, coasting \\ \dfrac{\sum_{i=1}^{8}\{u_b b(v_{ki}) + W_{ki}\}}{(1+\gamma)\sum_{i=1}^{8} m_{ki}} & cruising \end{cases} \quad (9)$$

For the energy-saving purpose in determining the traction strategy, an energy consumption model is basically required to evaluate the energy situations of a certain traction process. The energy consumption index J for a high-speed train can be calculated as

$$J = J_{\text{bas}} + J_{\text{aux}} \quad (10)$$

where J_{bas} is the basic traction energy derived by the traction actions, which correspond to the traction and cruising conditions, and J_{aux} represents the auxiliary energy component. These two components can be computed as

$$J_{\text{bas}} = \frac{1}{\varepsilon_1}\int f(v)v dt + \varepsilon_2 \int b(v)v dt \quad (11)$$

$$J_{\text{aux}} = \psi T \quad (12)$$

where ε_1 is the coefficient referring the conversion from the electric energy to the mechanical energy, ε_2 refers the conversion from the mechanical energy to the electric energy, ψ is the auxiliary power of the train, and T denotes the time consumption of the whole trip.

To determine the optimal train traction solution, the whole trip is divided into several sub-sections based on the speed limit, and the energy consumption of a sub-section $j(j \le N)$ can be evaluated as the corresponding conditions, where

$$J_j^{(\text{tra})} = \frac{\sum_{i=1}^{8} m_i}{3.6^3 \times 1000} \cdot \frac{(v_{\text{end},j}^2 - v_{\text{init},j}^2)}{2} \quad (13)$$

$$J_j^{(\text{cru})} = \frac{g}{3600}\left(s_{\text{cru},j} W_j \sum_{i=1}^{8} m_i \right) = \frac{g}{3600}\left\{ s_{\text{cru},j}\left[r(\bar{v}_j) + g(\bar{v}_j) \right] \sum_{i=1}^{8} m_i \right\} \quad (14)$$

where $J_{\text{tra},j}$ and $J_{\text{cru},j}$ are energy consumption for traction and cruising conditions in the j th sub-section, i means the number of train compartment, $v_{\text{init},j}$ and $v_{\text{end},j}$ denote the initial and target end speed of a sub-section, $\bar{v}_j$ is the average speed, and $r(\bar{v}_j)$ and $g(\bar{v}_j)$ are the basic resistance and the additional resistance with an average speed $\bar{v}_j$. For simplification purposes, the energy consumption for the braking and coasting conditions are set as $J_j^{(\text{brk})} = J_j^{(\text{coa})} = 0$.

Copyright ⓒ 2015 SERSC

According to the above analysis, when the condition of each sub-section is determined, the total energy consumption during a whole travel can be derived by using a summation, which is a solution to Eq. (10) as

$$J = \sum_{j=1}^{N} J_j^{(\eta_j)} + J_{\text{aux}} \tag{15}$$

where η_j represents the condition mode of section j, which belongs to $\{\text{tra}, \text{brk}, \text{coa}, \text{cru}\}$.

2.2. Optimization Traction Control with PSO

Different from the traditional traction control method using the single-particle EMU model, in this paper, the multi-mass EMU model is employed to ensure an effective description for traction operations. Under a target of energy-efficiency optimization, the energy consumption model can be used to estimate and determine a sequence of operation conditions and the corresponding condition conversion points. A condition sequence chain "traction-cruising-coasting-braking" is taken as the minimum unit to complete a whole trip. Besides that, speed limits determined by the rail track features (e.g. gradient, curvature, and signaling conditions). Uncertainty exists in the combination of operation condition sequences and the energy-saving target. Therefore, intelligent algorithms are introduced in this paper to determine an optimized solution of train traction control.

Due to the constraint from the speed limit condition, there are mainly two steps to calculate the optimized traction control solution: 1) determination of sub-sections; and 2) calculation of the condition sequence.

First, the determination of sub-sections is carried out according to the features of the track, including track length, speed limits and gradients. For the sub-section $j(j = 1, 2, \cdots, N)$ with a length $\bar{s}_j = |x_j - x_{j-1}|$ and the gradient $grad_j$, where x_j denotes longitudinal location of a train, the situation of speed limits $(\tilde{v}_{j-1}, \tilde{v}_j)$ between adjacent sub-sections may result in different strategies for the traction and operations. Figure 3 indicates the four situations.

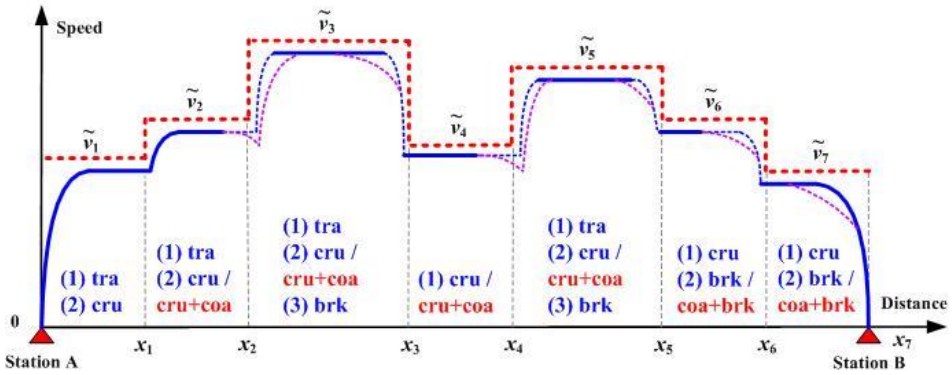

Figure 3. Operation Control Strategies under Different Speed Limit Situations

When the speed limits of all the sub-sections are determined, the following problem is to determine the sub-sequence of a traction strategy for each sub-section, which is an integration of the above mentioned four operation conditions. According to the principles as shown in the Figure 3, the solution of a j th sub-sequence is described by a set of speed indices, including the initial speed $v_{\text{init},j}$, target speed $v_{\text{tar},j}$, initial braking speed

 Copyright ⓒ 2015 SERSC

$v_{\mathrm{brk},j}$ and the end speed $v_{\mathrm{end},j}$. For the seven situations as shown in Figure 3, the pre-condition for calculating an optimized sequence is listed as follows.

$$j=\begin{cases}1, & v_{\mathrm{init},j}=0, v_{\mathrm{tag},j}\in(0,\tilde{v}_j], v_{\mathrm{end},j}\in(0,v_{\mathrm{tag},j})\\ 2, & v_{\mathrm{init},j}=v_{\mathrm{end},j-1}, v_{\mathrm{tag},j}\in(0,\tilde{v}_j], v_{\mathrm{end},j}\in(\tilde{v}_{j-1},v_{\mathrm{tag},j})\\ 3, & v_{\mathrm{init},j}=v_{\mathrm{end},j-1}, v_{\mathrm{tag},j}\in(0,\tilde{v}_{j+1}], v_{\mathrm{brk},j}\in(0,\tilde{v}_j), v_{\mathrm{end},j}\in(0,\tilde{v}_{j+1})\\ 4, & v_{\mathrm{init},j}=v_{\mathrm{end},j-1}=v_{\mathrm{tag},j}, v_{\mathrm{end},j}\in(0,v_{\mathrm{tag},j}]\\ 5, & v_{\mathrm{init},j}=v_{\mathrm{end},j-1}, v_{\mathrm{tag},j}\in(0,\tilde{v}_{j+1}], v_{\mathrm{brk},j}\in(0,\tilde{v}_j), v_{\mathrm{end},j}\in(\tilde{v}_{j+2},\tilde{v}_{j+1})\\ 6, & v_{\mathrm{init},j}=v_{\mathrm{end},j-1}, v_{\mathrm{tag},j}\in(0,\tilde{v}_{j+1}], v_{\mathrm{brk},j}\in(0,\tilde{v}_j), v_{\mathrm{end},j}\in(0,\tilde{v}_{j+1})\\ 7, & v_{\mathrm{init},j}=v_{\mathrm{end},j-1}, v_{\mathrm{tag},j}=0, v_{\mathrm{brk},j}\in(0,\tilde{v}_j), v_{\mathrm{end},j}=0\end{cases} \tag{16}$$

Second, by matching the situations as (16), the state vector $\hat{\boldsymbol{x}}_j=(v_{\mathrm{init},j},v_{\mathrm{tag},j},v_{\mathrm{brk},j},v_{\mathrm{end},j})^{\mathrm{T}}$ can be initialized and used for generating the optimized results. With the energy consumption model that is shown in Eq. (15), the energy efficiency of an operation sequence is a function of speed indices from $\{\hat{\boldsymbol{x}}_j\}$. However, it is difficult to determine a minimum-energy solution since we cannot directly build a theoretical description for $\{\hat{\boldsymbol{x}}_j\}$ and the object function $J_{\min}$. Therefore, the particle swarm algorithm is considered for solving the energy-saving problem, where the widely used PSO (Particle Swarm Optimization) technique is involved.

The PSO technique, which promises to provide an effective optimization capability with a simple implementation, is applied here to solve the optimization problem by using a single objective for minimizing the energy consumption. With the definition of the fitness function, the particle population is evaluated for determining the local and global optimization results. For the sub-section j, we use $\bar{\boldsymbol{x}}_j^{\mathrm{p}}$ and $\bar{\boldsymbol{x}}_j^{\mathrm{g}}$ to indicate local and global best locations. After initialization, the position $\boldsymbol{x}_j^l(i)$ and velocity $\boldsymbol{\mu}_j^l(i)$ of the particle l at the ith evolution step are defined for the iteration, where the population is with a constant value $N_{\mathrm{p}}(l\le N_{\mathrm{p}})$ and the iteration is infinite under certain termination conditions.

In each iteration step, the particles are updated as

$$\boldsymbol{\mu}_j^l(i)=\omega\boldsymbol{\mu}_j^l(i-1)+c_1r_1\left\{\bar{\boldsymbol{x}}_j^{\mathrm{p}}(i)-\boldsymbol{x}_j^l(i-1)\right\}+c_2r_2\left\{\bar{\boldsymbol{x}}_j^{\mathrm{g}}-\boldsymbol{x}_j^l(i-1)\right\} \tag{17}$$

$$\boldsymbol{x}_j^l(i)=\boldsymbol{x}_j^l(i-1)+\boldsymbol{\mu}_j^l(i) \tag{18}$$

where ω is the inertia weight, c_1 and c_2 denote the acceleration coefficients, and r_1 and r_2 are the parameters with random values.

By using the above principles to update the location and velocity of the particles, the global best location will gradually converge to the optimized value, on the basis of a suitable fitness function and the corresponding decision making logic. A constant target threshold $\bar{\rho}$ for the fitness is employed for terminating the iteration while the following criterion is fulfilled

Copyright ⓒ 2015 SERSC

$$\rho^l(i)\Big|_{x_j^l(i)=\bar{x}_j^g} \le \bar{\rho},\ j=1,2,\cdots,N \tag{19}$$

$$\rho^l(i)=J^l(i)=\sum_{j=1}^{N}\left\{J_j^{l,(\eta_j)}(i)+J_{\text{aux},j}^l(i)\right\} \tag{20}$$

which means the global best fitness is within the bound of a given threshold level.

In order to constrain the calculation to avoid infinite iterations without fulfilling criterion (20), an assistant principle for breaking the PSO calculation is involved by using a maximum iteration step L, which indicates that the PSO iteration will be terminated when the current step exceeds the threshold (as $i \ge L$) and the criterion (19) is not fulfilled for all the past steps ($i=1,2,\cdots,L-1$).

As an important branch of public transportation services, the modern high-speed railway is concerning more on the service quality. With a basis of safety, the passenger comfort is also a decisive factor for ensuring the service acceptance, which should also be considered in the design of the optimized train traction operation strategies. According to the dynamics of high-speed trains, the degree of discomfort could be evaluated by the integral

$$\psi^l(i)=\int\left|\frac{d\left[a^l(i)\right]}{dt}\right|dt=\sum_{j=1}^{N}\left|\Delta a_j^l(i)\right| \tag{21}$$

where $a^l(i)$ denotes the acceleration of a train for the particle l at step i, and $\Delta a_j^l(i)$ is the equivalent difference of $a^l(i)$ for each sub-section with different operation modes considered.

The value of $\psi^l(i)$ is inversely proportional to the comfort of passengers under the current traction control strategy, and hence, the optimization process should concern this restraint. Furthermore, the pre-condition for the train traction optimization should be considered due to the priori constraint from the operation planning of high-speed trains. Since the timetables for the trains have been designed before the operation activities, the optimization oriented to the energy efficiency or the passenger comfort should also take into account the constraint of the traveling time. The traveling time of a sub-section can be calculated as

$$T^l(i)=\int\frac{1}{F^l(i)}dv=\sum_{j=1}^{N}\int_{v_{\text{init},j}}^{v_{\text{end},j}}\frac{1}{F^l(i)}dv \tag{22}$$

where $F^l(i)$ denotes the resultant force of the train when the traction strategy from the l th particle is adopted.

Based on the above analysis, it can be seen that the several factors should be considered in the design of an optimized traction solution, which requires an effective optimization method that could provide certain coverage to these issues. Besides the multi-objective optimization techniques, the single-objective optimization is with its advantage in simplicity for pursuing the unique solution by PSO, where the design of the fitness function is a key factor. Here we can integrate the three objectives using a linear weighing strategy, and thus a fitness function that is applied for evaluating the particles can be re-written as the following form

 Copyright ⓒ 2015 SERSC

$$\tilde{\rho}^{l}(i)=\varpi_1\frac{J^{l}(i)}{\sigma_1}+\varpi_2\frac{\psi^{l}(i)}{\sigma_2}+\varpi_3\frac{T^{l}(i)}{\sigma_3} \tag{23}$$

where $\tilde{\rho}^{l}(i)$ represents the improved fitness for the particle l at step i, ϖ_1, ϖ_2 and ϖ_3 are the weight coefficients for tuning the fitness, σ_1, σ_2 and σ_3 are normalization coefficients.

The weight coefficients are decisive factors with the given models of these indices, since they can directly adjust the importance degrees of the three aspects under different scenarios. There can be the linear or nonlinear weight coefficient strategies for an enhanced fitness with the constraint $\varpi_1 \geq \varpi_2+\varpi_3$, such as $\varpi_1+\varpi_2+\varpi_3=1$ and $\varpi_1^2+\varpi_2^2+\varpi_3^2=1$. Value spaces of the two examples are shown in Figure 4.

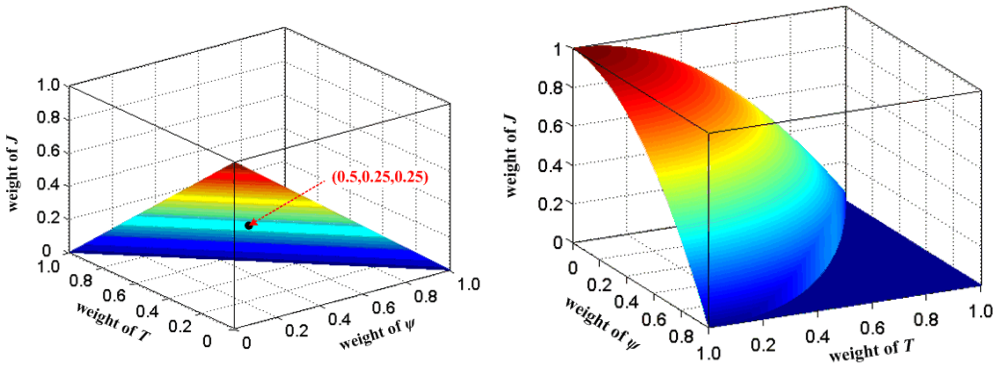

Figure 4. Value Spaces of Weight Coefficients (Left: Linear Strategy; Right: Nonlinear Strategy)

By using the terminating principle for PSO with a fitness limit $\bar{\rho}$ or a maximum step L, the speed indices for each sub-section are extracted from the particle with a global best fitness, and thus the whole trajectory of the high-speed train in the trip is derived. Based on the force model and the parameters of the EMU, the optimized traction control solution is obtained.

Algorithm 1. PSO-based train traction control solution.

Begin

1 Input the rail track parameters $\{\bar{s}_j, \bar{v}_j, grad_j\}$.

2 Determine the sub-sections and the corresponding pre-conditions according to Eq. (16).

3 ***loop***

4 Initialize the population of particles $\{\boldsymbol{x}_j^l, \boldsymbol{\mu}_j^l\}$ for a sub-section j.

5 Initialize the PSO parameters $\{\omega, c_1, c_2, r_1, r_2, \bar{\rho}, L, \varpi_1, \varpi_2, \varpi_3, \sigma_1, \sigma_2, \sigma_3\}$.

6 Set the local best $\{\bar{\boldsymbol{x}}_j^{\mathrm{p}}\}$ and global best $\{\bar{\boldsymbol{x}}_j^{\mathrm{g}}\}$ with the current position.

7 ***loop***

8 Update the particles $\{\boldsymbol{x}_j^l(i), \boldsymbol{\mu}_j^l(i)\}$ within one iteration step as Eq. (17) and (18).

9. Evaluate the fitness $\tilde{\rho}^{l}(i)$ of each particle as Eq. (23).

10. Update the local best fitness $\tilde{\rho}^{\mathrm{p}}(l)$ if $\tilde{\rho}^{l}(i) < \tilde{\rho}^{\mathrm{p}}(l)$.

11. Update the local best fitness $\tilde{\rho}^{\mathrm{g}}$ if $\tilde{\rho}^{\mathrm{p}}(l) < \tilde{\rho}^{\mathrm{g}}$.

12. If the condition $\tilde{\rho}^{\mathrm{g}} < \bar{\rho}$ or $i \geq L$ is fulfilled, exit loop.

13. ***end loop***

14. Determine the optimized state vector $\hat{\boldsymbol{x}}_j$ for sun-section j.

15. If all the sub-sections are calculated, exit loop.

16. ***end loop***

17. Calculate the optimized trajectory and operation condition sequences using $\{\hat{\boldsymbol{x}}_j\}$.

18. Calculate the traction control sequences $\{a_k^f\}$ as Eq. (9).

End

According to the above mentioned PSO principles for the energy-efficient traction control issue for high-speed trains, the calculation procedure to generate an optimized solution can be summarized as Algorithm 1. From the indicated procedure and pre-defined conditions, the optimized traction control solution can be derived by the off-line operations. The strategy for the weight coefficients in a particle fitness function promotes a compromise to comprehensive effectiveness under an original intention for the energy-efficient control.

3. Simulation and Analysis

In this section, in order to validate the performance of the proposed algorithm, simulations are carried out with practical track conditions and parameters of Beijing-Shanghai high-speed railway. The performances from different optimization methods are compared using specific EMU parameters. Three strategies for traction control optimization are involved:

(1) Conventional traction control without optimization.

(2) Optimized traction control using PSO with a single-objective-based fitness function.

(3) Optimized traction control using PSO with a multi-objective-based fitness function.

The length of the test track between two successive train stations is 158km, and the speed limits are pre-defined for the sub-sections as 300km/h, 200km/h and 300km/h respectively. The speed limits and gradient condition of the test track are shown in Figure 5.

 Copyright ⓒ 2015 SERSC

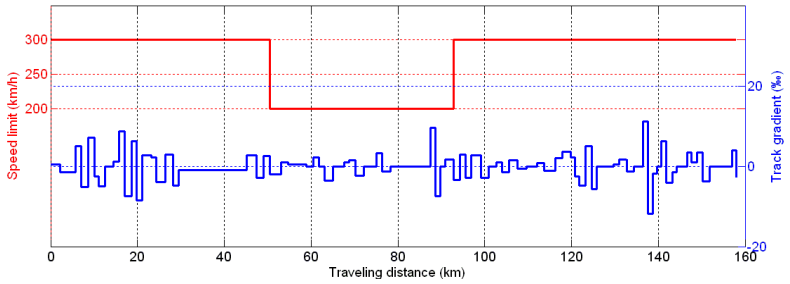

Figure 5. Speed Limits and Gradient Condition of the Track Section for Test

First, without any optimization operation, we analyze the train operation process according to the conventional CRH train traction calculation model and algorithms [15]. The parameters applied for the traction calculation are listed in Table 1.

Based on the obtained indices of the running process, the running curve of the whole trip is shown in Figure 6, which also depicts the switch of operation conditions and the acceleration of the train. To distinguish the different operation conditions, we use the values -1, 0 and 1 to represent the braking, intermediate and the traction conditions respectively. From the figures, it can be found that the derived traction control solution is capable of tracking the constraints of track conditions. Under a boundary operation scheme and the requirement of time planning, the conversion of operation conditions guarantees the fulfillment of the traffic principles and the EMU equipment characters. However, there are frequent switches of the control strategies during the intermediate conditions, and the value of acceleration is regularly fluctuated due to the idealization of track conditions and the identified operation strategies.

Table 1. Parameter Settings in Conventional Train Traction Calculation

Parameter	Value
EMU component mass m_{ki} (constant value) / t	52.5
Gravitational acceleration / m/s^2	9.81
Rotary mass coefficient γ	0.06
Basic resistance $r(v)$ / N/kN	0.79+0.0064v+0.000115v^2
Maximum braking force $b(v)$ / N/kN	81.55
Length of sub-section 1 $\overline{s}_1$ / km	50.5
Length of sub-section 2 $\overline{s}_2$ / km	42.38
Length of sub-section 3 $\overline{s}_3$ / km	65.17

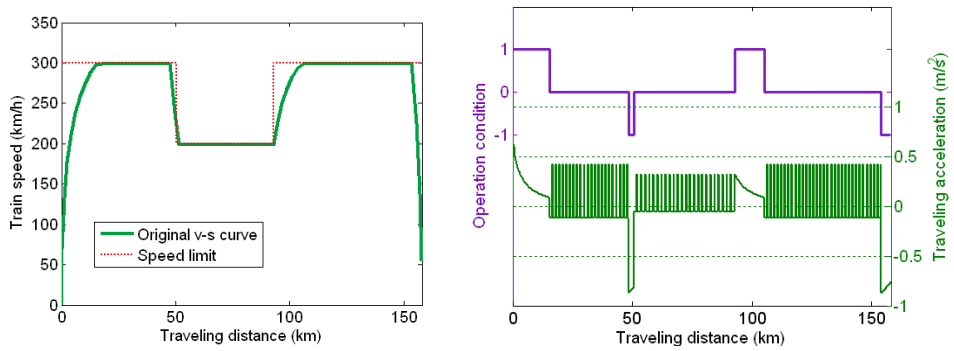

Figure 6. Results of Train Traction Calculation using the Conventional Method

Second, in order to validate the presented PSO-based optimization algorithm for the EMU traction control, the PSO-based optimization methods are performed with the single-objective fitness strategy, where three indices are tested separately, including the energy consumption, passenger comfort and the traveling time. The parameters used in the PSO-based calculations are listed in Table 2.

Table 2. Parameter Settings in the PSO-Based Calculation

Parameter	Value
Inertia weight ω	0.8
Acceleration coefficient c_1	1.494
Acceleration coefficient c_2	1.494
Particle population N_p	50
Maximum iteration step L	50
Value space of particle velocity $\boldsymbol{\mu}_j^l(i)$	[-0.5, 0.5]

Results from the single-objective-based PSO method are compared with the conventional traction strategy. Table 3 summarizes the results of the four strategies, where some additional indices are involved to evaluate the improvements. We use $\eta_J = [(J_0 - J)/J_0] \times 100\%$ and $\eta_\psi = [(\psi_0 - \psi)/\psi_0] \times 100\%$ to represent the improvement of energy consumption and the comfort, where the subscript '0' denotes results from the conventional strategy. ΔT indicates the deviation of the traveling time from the reference value.

Table 3. Results of the Conventional and Single-Objective-Fitness-Based PSO Solutions

Mode	Energy consumption		Discomfort		Time consumption	
	J	η_J	ψ	η_ψ	T	ΔT
Conventional traction	2837.4	-	81.521	-	2351	-
PSO with min $J^l(i)$	2388.7	15.81%	43.192	47.02%	2372	21
PSO with min $\psi^l(i)$	2432.1	14.28%	39.494	51.55%	2363	12
PSO with min $T^l(i)$	2447.6	13.74%	41.365	49.26%	2346	-5

From the comparisons, it can be found that the application of PSO technique provides great improvement to these indices over the conventional method. Within the same traction control scheme, the energy consumption is reduced to a certain extent by PSO optimization as well as the passenger discomfort. However, an increase of traveling distance becomes the expense for pursuing the energy and comfort targets. As the theoretical analysis, a balanced effectiveness of the optimization, under the premise of energy efficiency, is of great necessity. Hence, we further investigate the performance of a PSO-based calculation using a multi-objective fitness definition. A linear weight strategy with $[\varpi_1, \varpi_2, \varpi_3] = [0.5, 0.25, 0.25]$ as shown in Figure 4 is adopted for test and analysis. Figure 7 shows the results of fitness from each particle during the iterations, and the evolution of the global best fitness is illustrated. The results of traction control with

 Copyright ⓒ 2015 SERSC

the optimized solution are shown in Figure 8, where the speed-distance curve, operation condition and the traveling acceleration are all provided.

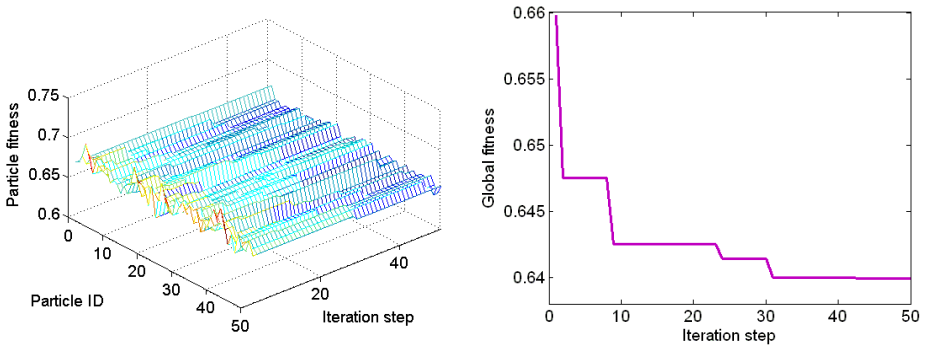

Figure 7. Particle Fitness and the Global Best Value during the Iterations

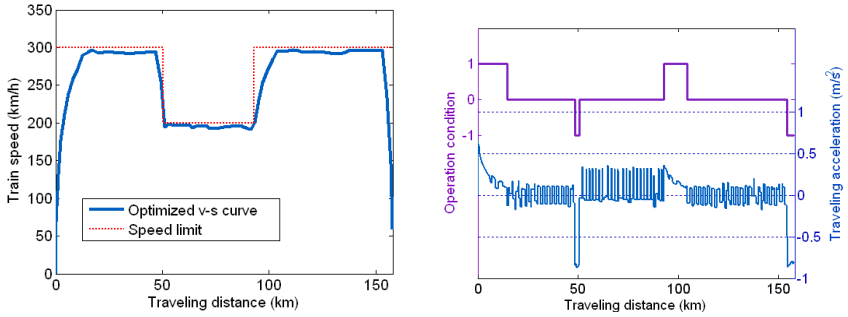

Figure 8. Results of Train Traction Calculation using the Multi-Objective-Fitness PSO

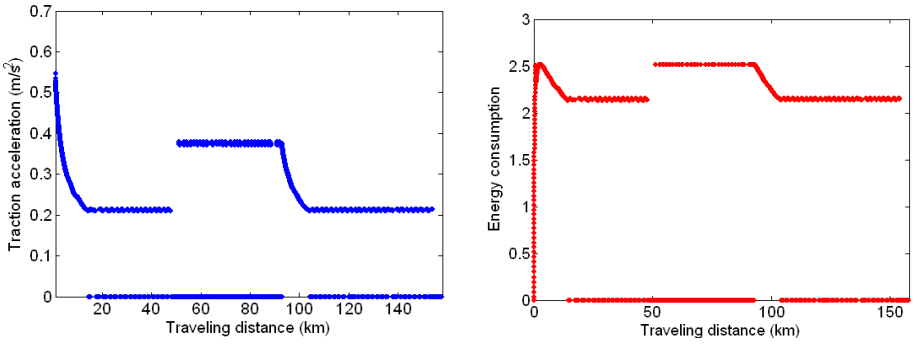

Figure 9. The Derived Traction Acceleration and the Corresponding Energy Consumption

Compared with the results in Figure 6, there is not great difference in condition conversion when the optimization strategy is adopted. However, the fluctuation of the train's acceleration is relatively eased, especially in the intermediate condition periods. Since coasting operations are involved and gradient constraints are concerned in the dynamic analysis of the resultant force, the derived speed profile is not as smooth as the ideal results. Consequently, the energy consumption is obviously reduced as the theoretical analysis. Figure 9 shows the required traction acceleration and the corresponding energy consumption with the traveling distance.

Copyright ⓒ 2015 SERSC

Table 4. Results of the Multi-Objective-Fitness-Based PSO Solutions

ϖ_1	ϖ_2	ϖ_3	Energy consumption		Discomfort		Time consumption	
			J	η_J	ψ	η_ψ	T	ΔT
0.5	**0.5**	**0**	2393.6	15.64%	41.869	48.64%	2373	22
0.5	**0**	**0.5**	2430.5	14.34%	41.839	48.68%	2353	2
0.5	**0.25**	**0.25**	2408.3	15.12%	42.466	47.91%	2364	13

To illustrate the effectiveness of the weighted fitness strategies, two strategies, which only consider the comfort or the running time, are involved for comparison and validation. Table 4 depicts the weights and the optimization results. All the three strategies take full advantages of the proposed multi-fitness definition, which provides notable improvements of the energy consumption (with a maximum of 15.64%) and the discomfort level (with a maximum of 48.68%). Particularly, the results converge as the distribution of $\{\varpi_i\}$. Overall, the traction energy consumption of a whole trip definitely decreases with the weight ϖ_1 in an integrated fitness function, and a longer traveling time will be derived in general.

4. Conclusions

In this paper, we have proposed a PSO-based algorithm for generating the traction control solution for high-speed trains. In this approach, the multi-mass EMU model enhances the analysis of the resultant force during the different operation conditions. Based on the energy consumption model, particle swarm optimization is enabled with an improved fitness strategy, where the additional performance indices, including the passenger comfort and traveling time, could be covered. By this method, the train traction control solution can be computed though a finite iteration process, and some additional values are achieved as well as energy efficiency. The simulation results show that the presented approach is capable of optimizing the traction control within an identified operation scheme. In the future work, an optimization concerning the train tracing scenarios and railway signaling constraints will be investigated. Furthermore, the operation control using extended equipment models is expected for further evaluations.

Acknowledgements

This research was supported by National Key Technology R&D Program of China (2013BAG24B02), International Science & Technology Cooperation Program of China (2014DFA80260), National Natural Science Foundation of China (61403021, U1334211), and the Fundamental Research Funds for the Central Universities (2014JBM003).

References

[1] M. Yin, L. Bertolini and J. Duan, "The Effects of the High-speed Railway on Urban Development: International Experience and Potential Implications for China", Progress in Planning. In press **(2014)**
[2] C. Sheng, Y. Liu, F. Lin, X. You and T. Q. Zheng, "Power Quality Analysis of Traction Supply Systems with High Speed Train", Proceedings of the 4th IEEE Conference on Industrial Electronics and Applications, **(2009)** May 25-27; Xi'an, China
[3] H. Yang, Y. Fu, K. Zhang and Z. Li, "Speed Tracking Control using an ANFIS Model for High-speed Electric Multiple Unit", Control Engineering Practice. 1, 23 **(2014)**

 Copyright ⓒ 2015 SERSC

[4] Y.V. Bocharnikov, A.M. Tobias and C. Roberts, "Reduction of Train and Net Energy Consumption using Genetic Algorithms for Trajectory Optimisation", Proceedings of IET Conference on Railway Traction Systems, **(2010)** April 13-15; Stevenage, UK
[5] S. Lu, S. Hillmansen, T.K. Ho and C. Roberts, "Single-Train Trajectory Optimization", IEEE Transactions on Intelligent Transportation Systems. 2, 14 **(2013)**
[6] T. Moritani and K. Kondo, "Basic Study on a Designing Method of the Traction Equipments to Save the Running Energy with an Optimization Method", Proceedings of International Conference on Electrical Systems for Aircraft, Railway and Ship Propulsion, **(2010)** October 19-21; Bologna, Italy
[7] X. Feng, "Optimization of Target Speeds of High-speed Railway Trains for Traction Energy Saving and Transport Efficiency Improvement", Energy Policy. 12, 39 **(2011)**
[8] X. Li, D. Wang, K. Li and Z. Gao, "A Green Train Scheduling Model and Fuzzy Multi-objective Optimization Algorithm", Applied Mathematical Modelling. 4, 37 **(2013)**
[9] Y. Sun, C. Cao and C. Wu, "Multi-objective Optimization of Train Routing Problem Combined with Train Scheduling on a High-speed Railway Network", Transportation Research Part C: Emerging Technologies. 44 **(2014)**
[10] S. Dundar and I. Sahin, "Train Re-scheduling with Genetic Algorithms and Artificial Neural Networks for Single-track Railways", Transportation Research Part C: Emerging Technologies. 27 **(2013)**
[11] R. Chen, L. Liu and J. Guo, "Optimization of High-Speed Train Control Strategy for Traction Energy Saving Using an Improved Genetic Algorithm", Journal of Traffic and Transportation Engineering. 1, 12 **(2012)**
[12] S. Sun, Y. Li and H. Xu, "Energy Consumption Optimization for High-speed Railway based on Particle Swarm Algorithm", Proceedings of 4th International Conference on Computational Intelligence and Communication Networks, **(2012)** November 3-5; Mathura, India
[13] J. Yu, Q. Qian and Z. He, "Study on Train Traction Simulation of High Speed Motor Train Set", Journal of the China Railway Society. 5, 30 **(2008)**
[14] X. Kang, "Study on Train Traction Simulation of High Speed Motor Train Set", Engineering Science. 1, 13 **(2011)**
[15] J. Peng, Editor, "Traction and Brake of Electronic Multiple Unit", China Railway Publishing House, Beijing **(2009)**

Copyright ⓒ 2015 SERSC

Copyright ⓒ 2015 SERSC